



Body Composition Assessments



Table of Contents

INTRODUCTION.....	3
BODY COMPOSITION MODELS AND CONCEPTS	4
REFERENCE METHODS OF ASSESSING BODY COMPOSITION.....	6
HYDRO-DENSITOMETRY	6
AIR DISPLACEMENT PLETHYSMOGRAPHY	9
DUAL-ENERGY X-RAY ABSORPTIOMETRY	12
DILUTION TECHNIQUES FOR ESTIMATING BODY WATER.....	14
ADDITIONAL BODY COMPOSITION METHODS	16
COMPUTED TOMOGRAPHY.....	16
MAGNETIC RESONANCE IMAGING.....	18
FIGURE 5. MAGNETIC RESONANCE IMAGING.	18
MAGNETIC RESONANCE SPECTROSCOPY.....	19
FIELD-BASED METHODS OF ASSESSING BODY COMPOSITION.....	20
SKINFOLD TECHNIQUE.....	20
BIOELECTRIC IMPEDANCE	22
ANTHROPOMETRY	24
BODY MASS INDEX	24
CIRCUMFERENCE METHODS	25
REFERENCES.....	28



Introduction

Historically the study of body composition has been restricted to either laboratory measurements, which make inferences established on a small sample cadaver analysis, or field tests, which through mathematical modelling make further assumptions based on the laboratory assessments. Unfortunately, the reliance on indirect measurements centred on these assumptions [i.e., formulated from restricted sample sizes] has added to a degree of ambiguity when evaluating and assessing body composition, specifically in populaces not included in some of the original cadaver studies (e.g., non-Caucasians, adolescents, and diseased people). Perhaps for this reason the application of body composition has been limited mostly to athletics and research.

Conversely, with the introduction of more accurate means of body composition measurement instruments such as dual-energy X-ray absorptiometry (DEXA), magnetic resonance imaging (MRI), or computed tomography (CT), we now can measure in vivo components that were formerly assumed. These developments have aided in generating new reference models, which has allowed better, more specific population extrapolation calculations. Some of these procedures have become common, such as DEXA, which is used to measure bone mineral density for disorders such as osteoporosis. Other areas show conceivable but remain under-utilised due to high costs and a lack of understanding. For example, the use of CT imaging in oncology to assess skeletal muscle loss. This is an important clinical marker correlated to disease progression and early death in individuals undertaking chemotherapy.

Body composition measures have been further used when it comes to one of the most prevalent and costly health disorders globally: obesity. According to contemporary data, more than 35% of males and females in the United States are considered obese, and almost 70% of all Americans are considered overweight. With a large body of evidence connecting obesity to various chronic health disorders, there is considerable emphasis given to developing and improving weight-loss procedures and approaches. When effective, weight loss has been shown to counteract, improve, or even improve certain chronic health conditions (e.g., diabetes, and hypertension).



Body Composition Models and Concepts

The fundamental suppositions of various body composition models still used today originate from investigations of three Caucasian male cadavers aged 25, 35, and 46 years. From the study of these bodies, Behnke et al., (1942) then later Brozek et al., (1963) and Siri (1956) established the two-component model, which divides the body into the amount of fat mass (FM) and fat-free mass (FFM). FFM is expressed as non-fat tissue (e.g., bone, muscle, organs, and connective tissue), while FM comprises energy reserves (e.g., visceral fatty deposits and subcutaneous fat) and essential fat.

The models of the three above research groups each assume that density for FM and FFM are constant, and that quantities of protein, water, and bone mineral are constant. Consequently, any change in body density (as measured by either underwater weighing or air displacement plethysmography) is attributed to alterations in FM. Intriguingly, both the Brozek and Siri equations, which are still applied today, generate similar percentage body fat values for individuals less than 30%. However, as stated, systemic errors happen with populations found to have different FFM densities (e.g., African Americans, Asians, and performance athletes). Established on more recent works, population-specific equations should be applied instead of the Brozek and Siri equations (**Table 1**).

Conventional body composition procedures such as underwater weighing using a two-component model, while current methods could measure individual elements at the atomic (e.g., carbon), molecular (e.g., protein), cellular (e.g., cell mass), and tissue (e.g., bone) levels. Integration of different body composition methods, one can develop the two-component model into a multi-component model. In the next few sections discussions around the DEXA as using a three-component model. An instance of a four-component model from Withers et al., (1999) would be the use of underwater weighing, isotopic dilution, and DEXA (i.e., body density, total body water, bone mineral density, and others). The key benefit of using a multi-component model is that sections such as total body water or bone mineral, which can vary from the assumed two-component model, can be reported. The shortcomings are that each method in a multi-component model has a distinct measurement error that is additive for each



measurement applied; this is acknowledged as the propagation of errors (Heyward and Wagner, 2004).

Table 1. Ethnicity-Specific Two-Component Equations for Converting Body Density (Db) to Percentage Body Fat.

Population Group	Age (years)	Conversion Formula	
		Males	Females
African American	9-17	-	$(5.24/D_b) - 4.82$
	19-45	$(4.86/D_b) - 4.39$	-
	24-79	-	$(4.86/D_b) - 4.39$
American Indian	18-62	$(4.97/D_b) - 4.52$	$(4.81/D_b) - 4.34$
Japanese	18-48	$(4.97/D_b) - 4.34$	$(4.76/D_b) - 4.28$
	61-78	$(4.87/D_b) - 4.41$	$(4.95/D_b) - 4.50$
Singaporean	61-78	$(4.94/D_b) - 4.48$	$(4.84/D_b) - 4.37$
Caucasian	8-12	$(5.27/D_b) - 4.85$	$(5.27/D_b) - 4.85$
	13-17	$(5.12/D_b) - 4.69$	$(5.19/D_b) - 4.76$
	18-59	$(4.95/D_b) - 4.50$	$(4.96/D_b) - 4.51$
	60-90	$(4.97/D_b) - 4.52$	$(4.97/D_b) - 4.52$
Hispanic	20-40	$(4.87/D_b) - 4.41$	-

Adapted, from the work of Heyward and D. Wagner, 2004.

Reference Methods of Assessing Body Composition

Though no gold standard for measuring body composition presently exists, the three frequently applied methods that are viewed as being most accurate and are used as reference methods are (i) hydro densitometry (i.e., underwater weighing), (ii) air displacement plethysmography (commercially identified as the Bod Pod), and (iii) DEXA.

Hydro-densitometry

The roots of hydro-densitometry (also identified as under-water weighing or hydrostatic weighing) date back to Archimedes, who was given the task of deciding whether a king's crown was made of pure gold. His discovery was when he recognised that the volume of an object was equal to the volume of displaced water when that object was placed in it. An easy way to understand this principle is if you think about how your favourite soft drink rises in a glass when you add ice. If the crown were made exclusively of gold, its density would be the same as that of pure gold. Centuries later, Behnke et al., (1942) established a method for measuring density in humans using the same principle as Archimedes.



Figure 1. Underwater weighing.

Underwater weighing (**Figure 1** above) is a two-component model that applies Archimedes' principle of water displacement to establish an individual's FFM and FM.



This principle states that the weight of an individual outside of water subtracted by the weight of an individual in water is equal to the volume of water that is displaced.

Underwater Equation

- $Db = m/V$

Where Db = body density; m = weight in air; and V = Volume

Hydro Densitometry Body Density Equation

- $\text{Body density} = \text{weight in air} / (\text{weight in the air} - \text{weight in water})$

Body density then can be applied to compute FFM and FM. This is because we know the density of fat (0.9007 g/cc) and fat-free body density (FFBd) (1.1000 g/cc). Variances in the assumed FFBd account for several population-specific equations (**Table 1**). When matched with the density of water, which differs with temperature but is close to 1.0 g/cc, it becomes apparent why people with a greater percentage of FM float and those with more muscle mass do not. Though, body density must be translated to FFM using one of the known population-specific equations such as the ones developed by Siri (1956).

When undertaking underwater weighing, adjustments are also required for the pockets of air remaining in the lungs and gastrointestinal tract. Since air confined in the gastrointestinal tract is much smaller (matched with air in the lungs) and cannot be measured directly, it is 0.1 litres. Air in the lungs is significant and can lead to considerable errors if an individual does not exhale entirely. Encouraging an individual to completely exhale is both a challenge and a constraint of the hydrostatic method. However, even when an individual exhales completely, a quantity of air known as the residual volume (RV) cannot be exhaled. The RV must be estimated, preferably using dilution methods such as helium dilution. If dilution methods are not accessible, RV can also be calculated by measuring the vital capacity and multiplying by 0.34 in males and 0.28 in females. Moreover, prediction equations for RV based on age, gender, and weight exist; however, these can have significant errors of up to 3.9%. Equally,



when RV is measured, the range for a true value is around $\pm 1.2\%$. This could mean the difference in accurately communicating that an individual's body fat is between 20% and 22.4% with measured RV or between 20% and 27.8% when RV is estimated.

Air Displacement Plethysmography

When air displacement plethysmography (also known as the Bod Pod, **Figure 2**) is compared with underwater weighing, it produces equivalent assessments of an individual's percentage of body fat. Though, unlike underwater weighing, one advantage of air displacement plethysmography is that it requires little effort from the individual or tester. Collins and associates (1999) stated that the technical error of measurement (i.e., the difference in measurement from one tester to another) is fundamentally insignificant at only 0.448%. An additional advantage of air displacement plethysmography is the time needed for testing. For example, Lockner et al., (2000) that the Bod Pod took on average 1 hour less to measure body fat when compared with underwater weighing in a group of children aged 10 to 18 years. Due to these benefits, the use of the Bod Pod has become common across various populations.



Figure 2. The Bod Pod.

Air displacement plethysmography is also like underwater weighing in that it establishes body volume to compute FM and FFM from body density. Though, as the name intimates, air displacement plethysmography measures the volume of air displaced as an individual sits inside a chamber that contains a known volume of air. This is completed in part by applying Boyle's law ($P_1V_1 = P_2V_2$), which states that at a constant temperature, the alteration in pressure is inversely correlated to the change



in volume. A practical example of Boyle's law is how air bubbles from a scuba diver get larger as they advance towards the surface. The volume of the bubble expands due to the decrease in water pressure as the bubble approaches the surface. Therefore, by knowing the volume of air in the unoccupied Bod Pod and measuring the change in pressure as a person sits inside, you can explain the volume of the individual. However, because an individual is not isothermic and because Boyle's law requires a constant temperature, the Bod Pod also needs to correct for fluctuations in temperature and humidity produced by an individual (Fields et al., 2002). Like underwater weighing, once an individual's body volume is known, this can be translated into body density and then percentage body fat using the same calculations used with underwater weighing.

Notwithstanding these clear benefits, careful consideration is required regarding procedures to evade prediction errors. As discussed before, the Bod Pod measures volume based on variations in pressure when an individual is placed in the chamber. However, because the chamber temperature is adiabatic (i.e., the temperature and pressure change because body heat is released), Poisson's law of pressure (a modification of Boyle's law) is applied to measure volume when the temperature is not constant ([Poisson's Law Equation below](#)) (Fields et al., 2002).

Poisson's Law Equation

- $P_1 / P_2 = (V_2 / V_1)^\gamma$

Where P = pressure; V = volume; and γ = ratio of the specific heat of the gas at a constant pressure to that at constant volume.

A typical error linked with the Bod Pod transpires when nonisothermic items (e.g., clothing, hair, jewellery) and air in the lungs falsely reduce body volume, which leads to an underestimation of body fat (Heyward and Wagner, 2004). To reduce these errors, close-fitting spandex shorts or swimsuits and a swim cap must be worn. To account for the volume of air in the lungs during normal tidal breathing, the Bod Pod measures thoracic gas volume. When thoracic gas volume is measured, an individual breathes routinely into a tube for several seconds. Then, the tube is briefly obstructed, and the individual is requested to give two or three moderate breaths. If the calculation



of thoracic gas volume is not within the tolerable range after three attempts, the Bod Pod software instead uses an estimated measure of thoracic gas volume.



Dual-Energy X-Ray Absorptiometry

It can be debated that DEXA (**Figure 3**) is not a three-component model but instead two separate two-component models. This is because DEXA computes separate segments of the body containing only soft tissue mass (i.e., fat and lean) and segments containing both soft tissue and bone (**Table 2**). These computations are established on the absorption of two distinct X-ray beams that differ depending on the maker (e.g., 40 and 70 keV). The two rays are needed when extrication tissue is inhomogeneous (i.e., containing distinctive components such as bone and soft tissue). Founded on recognised absorptions of lean and fat tissue, DEXA initially measures and computes the percentage of fat and lean tissue in the segments bereft of bone. Afterwards, centred on the identified absorptions of bone and soft tissue, DEXA does the same in the areas containing bone and soft tissue. Since fat and lean tissue are not directly measured in the areas containing bone, DEXA assumes the proportion of fat and lean tissue in the soft tissue mass around the bone to be the same as what was calculated in the regions without bone.

Table 2. Individual Components Calculated From DEXA.

Soft Tissue	Bone and Soft Tissue	
Fat + lean tissue mass	Fat + lean tissue mass (composition assumed based on bone-free scan) *	= Total tissue mass (i.e., fat + lean + bone)
	Bone mineral mass	
*Estimated from a scan of soft tissue only.		

When compared with underwater weighing, DEXA requires limited effort from the clients and takes only a few minutes to complete. An additional benefit is that DEXA can measure fat and muscle allocation in local areas of the body (e.g., the trunk and extremities). While radiation exposure is a shortcoming, the quantity is minimal as is equal to that of a cross-continental aeroplane flight.

DEXA is acknowledged as a reference model since of its precision compared with underwater weighing and multi-component models. Causes of error include incorrect body positioning, hydration status, the disparity between measured weight

and DEXA weight, and food intake (Pierson, Wang, and Thornton, 2000). An additional shortcoming of DEXA is the failure to assess clients with a large body mass index (BMI). Early-model DEXAs had a weight restriction of only 118 kg, while newer models have parameters of up to 180 kg. Difficulties ascend if an individual does not entirely fit within the examining field (Hangartner et al., 2013). While not optimum, offset scanning can be performed; this is where non-scanned areas are “imaged” by the computer to calculate the omitted segments (Hangartner et al., 2013).

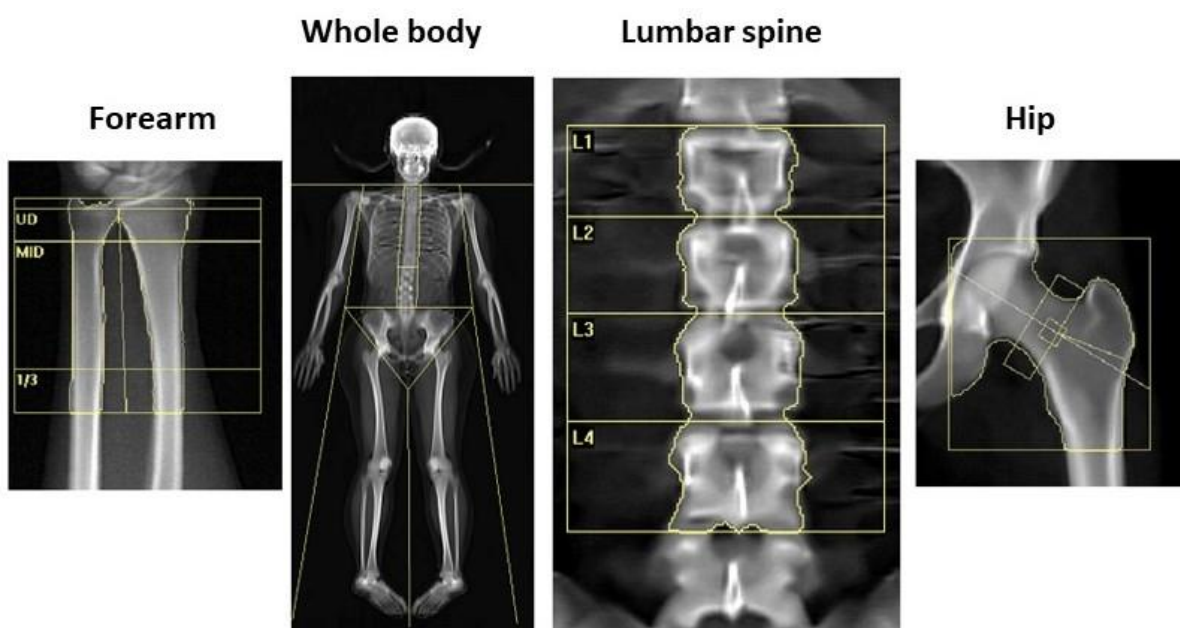


Figure 3. Dual-energy X-ray absorptiometry.



Dilution Techniques for Estimating Body Water

As previously discussed, FFM in the human adult contains almost 73% water. Remarkably, this amount of water to FFM is similar not only across humans but also in other animal species. Hydrometry is an alternative two-component model that measures total body water. FM and FFM can be estimated based on the known relationship between total body water and FFM.

The equation for Estimating Body Water

- $FFM = TBW/0.732$
- $\%BF = [BM - (TBW/0.732)]/BM \times 100$

Where FFM = fat-free mass; TBW = total body water; BM = body mass; and %BF = percentage body fat.

Hydrometry is established on the dilution principle that employs an isotopic tracer (e.g., tritium, deuterium) and measures the tracer in a diluted solvent (i.e., total body water). Providing the concentration of the tracer in the solvent is known and the original amount of tracer is identified, then the volume of the solvent (i.e., total body water) can be calculated. Like the other two-component models, hydrometry involves assumptions that can lead to error.

These assumptions are as follows:

1. Lean body mass (LBM) contains 73.2% water. Though, differences can happen in some individuals, specifically in diseased populations (e.g., heart failure, end-stage kidney disease), who can have large disparities in total body water.
2. The tracer diffuses evenly and completely through the total body water. Although this is mainly true, some amounts of tracer can be absorbed in body tissue (e.g., adipose tissue).



3. The tracer is not metabolised. Again, this is largely true for common tracers used currently.

4. The method for hydrometry comprises an over-night fast, a criterion body fluid sample (saliva, urine, or blood), administration of a recognised dose of an isotopic tracer, an equilibrium period (usually 3-4 hours), a second body fluid sample, and measurement of the isotope concentration in the body fluid (e.g., mass spectroscopy). Because hydrometry measures total body water, it is often used as part of a multicomponent model.



Additional Body Composition Methods

The capacity to measure fat and muscle allocation in distinctive areas of the body can provide essential evidence about associated health risks beyond whole-body composition procedures. Three methods that have altered the area of body composition inquiry are CT, MRI, and magnetic resonance spectroscopy. While these methods are costly to manage, each is extremely consistent and reproducible (Goodpaster, 2002).

Computed Tomography

When an X-ray travels through a segment of the body, a two-dimensional image of that X-ray will present as either dark or light conditional on the attenuation of the object. For instance, bone is denser than lung tissue. When taking a chest X-ray, more of the X-ray is absorbed in the ribs, creating a white appearance. Equally, the lungs appear black because more of the photon elements travel through them. However, a drawback of a regular X-ray is the intersecting of various tissues and organs, which inhibits the capacity to distinguish these components.



Figure 4. Computed Tomography.



In the 1970s, Hounsfield established a procedure in which to use a computer to restructure multiple images taken 180° around an object. The reconstructed images offered high-contrast pixel attenuations acknowledged as **Hounsfield units**. Since X-rays travel through body tissue differently depending on the density of that tissue, the CT scan can separate fat and muscle tissue. The first total-body composition measure taken was performed in 1984 at the University of Gothenburg. The introduction of CT has generated a greater understanding of fat distribution, specifically the significance of abdominal fat. Both the CT and MRI have revealed how increased fat in the viscera contributes to diabetes, heart disease, and liver disease (Goodpaster, 2002). One illustration of where research has led to clinical application is the diagnosis of fatty liver disease. CT scans of the liver produce an attenuation value; the less attenuation of the liver (measured in **Hounsfield units**), the greater the amount of fat in the liver.

Magnetic Resonance Imaging

One of the main downsides of the CT scan is exposure to ionizing radiation. Due to this, the CT scan may not be the best choice when needing to execute several assessments or when analysing children. However, MRIs, do not use ionizing radiation and instead are founded on the interaction of hydrogen protons with a magnetic field controlled by the MRI (Pietrobelli, Wang, Formica, and Heymsfield, 1998). Similar to CT, MRIs produce whole-body images that show the distribution of adipose tissue throughout the body (**Figure 5**). MRIs can also be applied regionally and have been reported to be sensitive to identifying body composition changes (e.g., increased muscle mass with training) over time. MRIs have also offered precise measures of extra muscular adipose tissue (**EMAT**), which is the fat that is visible on MRI images between muscle groups and beneath the muscle fascia. The amount of EMAT in a client is a superior predictor of insulin resistance than subcutaneous fat.



Figure 5. Magnetic Resonance Imaging.

Magnetic Resonance Spectroscopy

Magnetic resonance spectroscopy (MRS) can measure concentrations of atomic and metabolic elements in vivo; these elements are not assessable in any other way. MRS measures the resonance (normally of hydrogen atoms) and is conducted using the same equipment as the MRI. Comparable to MRI and CT scans, MRS has various functions outside of body composition (e.g., measuring neurotransmitters and metabolites in the brain) (**Figure 6**). A particular focus of interest in body composition is the occurrence of ectopic fat. Ectopic fat is stated as deposits of triglycerides not situated in adipose tissue (e.g., muscle, liver, and the heart). The manifestation of ectopic fat inside the myocyte (i.e., intramuscular adipose tissue) is linked with insulin resistance and diabetes.

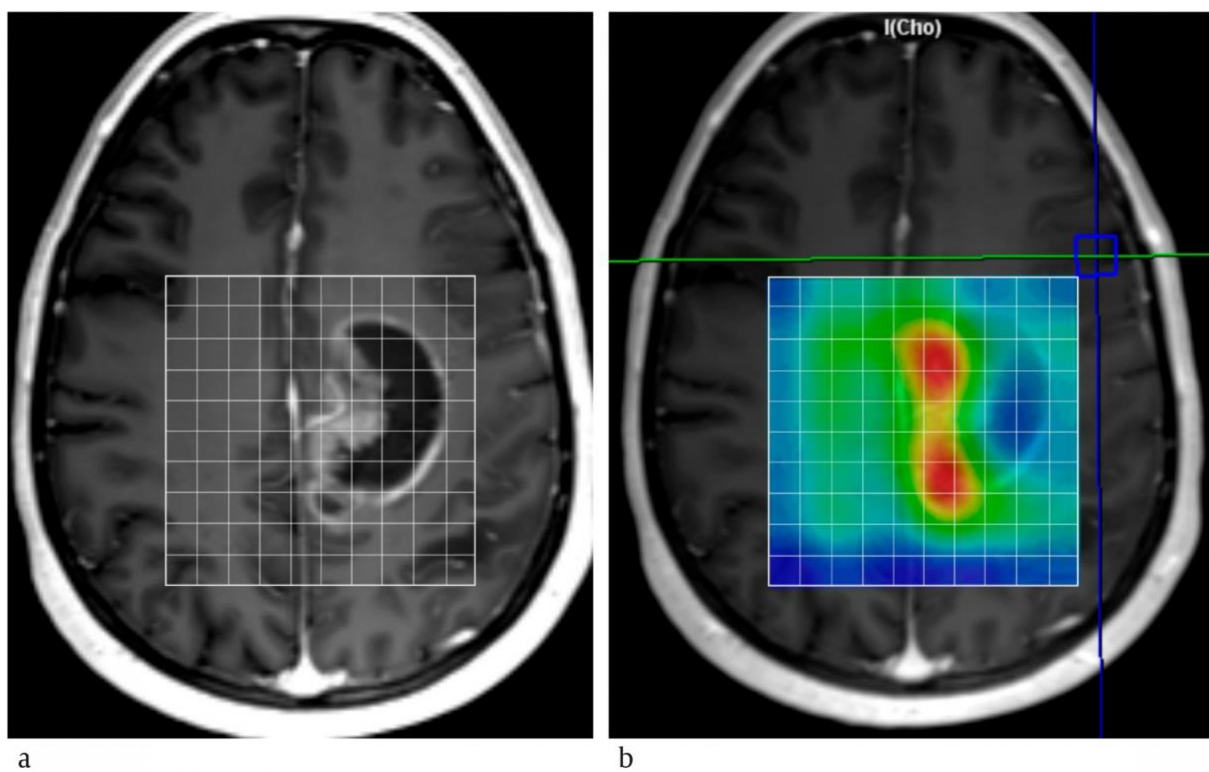


Figure 6. Magnetic Resonance Spectroscopy of the Brain.



Field-Based Methods of Assessing Body Composition

Due to the cost and practical provision of the earlier stated reference models, various specialists use field tests to assess subjects' body composition. Usually, these assessments use regression equations founded on the relationship of the field test measures to a reference model (e.g., hydro densitometry). The two field tests most applied are the skinfold method and bioelectric impedance.

Skinfold Technique

The skinfold method involves the use of skin callipers to measure subcutaneous fat directly underneath the skin. Subcutaneous fat composes 40% to 60% of total body fat and is associated with the body's internal fat stores. When the skinfold measures are acquired, these are inputted into a prediction equation to determine FM and FFM.

While the skinfold technique provides an effective and economical option for appraising the client's percentage of body fat, a key shortcoming is an estimated error of 3% to 11% (Heyward and Wagner, 2004). This error largely is due to the proficiency of the individual administering the skinfold test but can also be attributable to the use of unsuitable prediction equations (e.g., using an adult prediction equation when testing adolescents). Out of the various equations established, the Jackson and Pollock general equation is the most used. Established in the 1970s, the Jackson and Pollock equations for males and females used a quadratic regression equation established on underwater weighing (Jackson and Pollock, 1978; 1980).

- Females: $Db = 1.099421 - 0.0009929 (X1) + 0.0000023 (X1)^2 - 0.0001392 (X2)$
- Males: $Db = 1.10938 - 0.0008267 (X1) + 0.0000016 (X1)^2 - 0.0002574 (X2)$

Where Db = body density (percentage body fat can be converted using a two-component equation—e.g., Siri); $X1$ = sum of triceps, iliac crest, and midthigh skinfolds (females) or sum of the chest, abdominal, and midthigh skinfolds (males); $X2$ = age (rounded to the nearest year).



Recently, Nevill and colleagues (2008) reported that the generalised equation is a valid measurement that displays a high correlation with DEXA-derived percentage body fat ($r = .87$ for women; $r = .95$ for men). The main disadvantage of the generalized equation, however, was the cohort, which comprised largely of non-Hispanic Caucasians. O'Connor et al., (2010) noted that this led to systematic error in several ethnic population groups. Due to these limitations, O'Connor and associates developed an upgraded sum of skinfold equations established on a diverse group. Instead of comparing the sum of skinfolds to underwater weighing, the author's equations used DEXA as a reference model and integrated BMI. The benefits of these equations are ethnic-specific, have good agreement with DEXA (3.6% in females and 3.1% in males), and do not involve the use of an additional equation to convert body density into percentage body fat. The disadvantage is that the populace used was between 18 and 35 years, and consequently, the equations are not appropriate for ageing populations. Additionally, Nevill et al., (2008) noted that when using generalised skinfold equations, the percentage of body fat is drastically miscalculated in obese populations when the sum of skinfolds is greater than 120 mm.

O'Connor's Updated Skinfold Equations

- **Caucasian females:** $\%BF = (0.169 \times X_1) - (0.0007 \times X_1^2) + (0.849 \times BMI) + 1.260$.
- **Hispanic females:** $\%BF = (0.169 \times X_1) - (0.0007 \times X_1^2) + (0.849 \times BMI) + 3.146$.
- **African American females:** $\%BF = (0.169 \times X_1) - (0.0007 \times X_1^2) + (0.849 \times BMI) - 0.078$.
- **Caucasian and Hispanic males:** $\%BF = (0.190 \times X_1) - (0.0005 \times X_1^2) + (0.604 \times BMI) - 5.377$.
- **African American males:** $\%BF = (0.206 \times X_1) - (0.0005 \times X_1^2) + (0.604 \times BMI) - 1.987$.

Where %BF = percentage body fat; X_1 = sum of triceps, iliac crest, and midhigh skinfolds (females) or sum of the chest, abdominal, and midhigh skinfolds (males); BMI = body mass index.



Bioelectric Impedance

Bioelectric impedance is a fast and simple technique of estimating total body water by measuring the impedance (Z) of a small current as it travels through the body. Impedance is a function of both resistance (R), which is the amount a current is stopped as it endeavours to pass through an object, and reactance (X_c), which is the amount a current is reduced as it passes through an object: ($Z = R + X_c$). You could use impedance to measure the volume of a tube filled with a salt solution using this equation:

- $V = \rho L^2 / Z$

Where V is volume; ρ is the specific resistivity of a solution; and L is the length of the tube (i.e., cm) where the electrodes are positioned.

These principles and formulas are applied to establish total body water in humans. Though, our body is not a cylinder but rather five different-shaped cylinders: the arms, the legs, and the trunk. Bioelectrical impedance analysis (BIA) employs prediction equations to determine total body water. One example of this is a simple linear regression equation established by Lukaski et al., (1985) that used deuterium dilution as the reference model (total body water = $0.63 \times \text{height}^2 / R + 2.03$; $r = .95$).

Since FFM contains most of the body water, the impedance measured in a lean individual will be much less than in someone with a higher percentage of body fat. Once total body water is identified, FFM can be calculated using this equation:

- $\text{FFM (kg)} = \text{total body water (kg)} / 0.73$.

Therefore, a major assumption used in BIA is that FFM contains 73% water.

Conventionally, BIA is measured at the whole-body level using a single frequency (50 kHz) that passes between four electrodes placed on the right side around the wrist and ankles. Recently, several BIA models measured multifrequency impedances that can distinguish intracellular and extracellular water in addition to total body water (Kyle et al., 2004). This is because at a frequency of 50 kHz, the electricity



passes through the path of least resistance (i.e., around cell membranes), which would be the extracellular water, but at higher frequencies, the current travels through cell membranes, in theory yielding the intracellular water.

If the fundamental assumptions are met, BIA can be a good predictor of body fat. As with the other body composition methods, it is critical that we ascertain conceivable sources of error and, when accessible, use equations that account for variances in sex, age, physical status, and ethnicity. When using BIA, the main assumption is the euhydration of subjects. Because of this, individuals with electrolyte irregularities or fluid imbalances (e.g., congestive heart failure, end-stage kidney disease) may have false outcomes. However, even with euhydrated individuals, the assumption that lean body mass contains 73.2% water can differ independently. Das and associates (2003) reported that subjects with grade 3 obesity (BMI >40 kg/m²) had a greater percentage of lean body mass water (i.e., 75.6%) compared with the reference value.



Anthropometry

Anthropometry is the measurement of the size and proportion of the human body and is commonly used to estimate body fatness or risk linked with excess body fat. The most common measurement used is BMI (**Table 3**).

Body Mass Index

BMI is calculated by dividing body weight in kilograms by metres squared:

- $BMI = \text{kg}/\text{m}^2$.

BMI is simple to use, economical and can be measured across a large populace. Although BMI is highly correlated with adipose tissue ($r = .82$), it is not a complete replacement for body fatness. Across the general population, a BMI greater than or equal to $30 \text{ kg}/\text{m}^2$ is linked with higher mortality (Flegal et al., 2013). However, mortality follows a U-shaped curve, with the highest risk of mortality in people with BMIs lower than $18.5 \text{ kg}/\text{m}^2$ and higher than $35 \text{ kg}/\text{m}^2$. The reasons why individuals in the overweight (i.e., BMI of $25\text{-}29.9 \text{ kg}/\text{m}^2$) and grade I obesity (i.e., BMI of $30\text{-}34.9 \text{ kg}/\text{m}^2$) categories do not fall into a higher risk category is unclear, although it may either suggest a protective effect with some excess adipose tissue or simply be a limitation of using BMI.

Table 3. Body Mass Index Classifications.

Classification	Value (kg/m^2)
Underweight	<18.5
Normal weight	18.5-24.9
Overweight	25-29.9
Grade 1 obesity	30-34.9
Grade 2 obesity	35-39.9
Grade 3 obesity	>40



Circumference Methods

Circumference measures have been suggested as an alternative or an addition to BMI. Circumference measures have suitable consistency and can be applied to very large clients and are fast and economical to execute. However, the benefit of circumference measures, particularly when compared with BMI, is that they can provide data on fat distribution. Growing evidence shows that individuals who are shaped like an apple are at greater risk for chronic diseases including diabetes, hypertension, and heart disease. Moreover, reductions in waist circumference are linked with improved insulin sensitivity, reduced visceral fat (i.e., intra-abdominal fat), and decreased risk of diabetes. Waist circumference should be measured during exhalation with a flexible elastic tape measured perpendicular to the floor. The anatomical sites commonly used to measure waist circumference are as follows:

- At the umbilicus
- Above the iliac crest
- At the narrowest point between the last rib and the iliac crest
- Below the lowest rib
- At the midpoint between the last rib and the iliac crest

Wang et al., (2003) compared four waist circumference sites (the umbilicus was excluded) and found that all sites had good repeatability (intraclass correlation = 0.996) and were related to body fat. Though, the site just above the iliac crest had the highest correlation to body fat ($r = .89$ for females; $r = .60$ for males) compared with the other sites.

**Table 6.** Sites for Circumference Measurements.

Site	Anatomical Reference	Position	Measurement
Neck	Laryngeal prominence	Perpendicular to the long axis of the neck	Apply the tape with minimal pressure just inferior to the Adam's apple.
Shoulder	Deltoid muscles and acromion processes of scapula	Horizontal	Apply tape snugly over maximum bulges of the deltoid muscles, inferior to acromion processes. Record measurement at end of normal expiration.
Chest	Fourth costosternal joints	Horizontal	Apply tape snugly around the torso at the level of the fourth costosternal joints. A record at end of normal expiration.
Waist	The narrowest part of the torso, level of the "natural" waist between ribs and iliac crest	Horizontal	Apply tape snugly around the waist at the level of the narrowest part of the torso. An assistant is needed to position the tape behind the client. Measure at end of normal expiration.
Abdominal	The maximum anterior protuberance of the abdomen, usually at the umbilicus	Horizontal	Apply tape snugly around the abdomen at the level of the greatest anterior protuberance. An assistant is needed to position the tape behind the client. Take measurements at end of normal expiration.
Hip (buttocks)	Maximum posterior extension of buttocks	Horizontal	Apply tape snugly around the buttocks. An assistant is needed to position the tape on the opposite side of the body.
Thigh (proximal)	Gluteal fold	Horizontal	Apply tape snugly around the thigh, just distal to the gluteal fold.
Thigh (mid)	Inguinal crease and proximal border of the patella	Horizontal	With the client's knee flexed 90° (right foot on bench), apply tape at the level midway between the inguinal crease and proximal border of the patella
Thigh (distal)	Femoral epicondyles	Horizontal	Apply tape just proximal to the femoral epicondyles.
Knee	Patella	Horizontal	Apply tape around the knee at mid-patellar level with the knee relaxed in slight flexion.
Calf	The maximum girth of the calf muscle	Perpendicular to the long axis of the leg	With the client sitting on the end of the table and legs hanging freely, apply tape horizontally around the maximum girth of the calf.
Ankle	Malleoli of tibia and fibula	Perpendicular to the long axis of the leg	Apply tape snugly around the minimum circumference of the leg, just proximal to the malleoli.



Arm (biceps)	Acromion process of scapula and olecranon process of ulna	Perpendicular to the long axis of the arm	With the client's arms hanging freely at the sides and palms facing thighs, apply tape snugly around the arms at the level midway between the acromion process of scapula and olecranon process of the ulna (as marked for triceps and biceps skinfolds).
Forearm	The maximum girth of the forearm	Perpendicular to the long axis of the forearm	With the client's arms hanging down and away from the trunk and forearm supinated, apply tape snugly around the maximum girth of the proximal part of the forearm.
Wrist	Styloid processes of radius and ulna	Perpendicular to the long axis of the forearm	With the client's elbow flexed and forearm supinated, apply tape snugly around the wrist, just distal to the styloid processes of the radius and ulna.



References

- Behnke A, Feen B, Welham W. The specific gravity of healthy men. *J Am Med Assoc.* 1942; 118:495-8.
- Brozek J, Grande F, Anderson J, Keys A. Densitometric analysis of body composition: revision of some quantitative assumptions. *Ann NY Acad Sci.* 1963; 110:113-40.
- Siri W. The gross composition of the body. In: Tobias C, Lawrence J, editors. *Advances in biological and medical physics.* New York: Academic Press; 1956. p. 239-280.
- Withers RT, Laforgia J, Heymsfield SB. Critical appraisal of the estimation of body composition via two-, three-, and four-compartment models. *Am J Hum Biol.* 1999;11(2):175-85.
- Heyward V, Wagner D. *Applied body composition assessment.* 2nd ed. Champaign, IL: Human Kinetics; 2004.
- Collins M, Millard-Stafford M, Sparling P, Snow T, Rosskopf L, Webb S, et al. Evaluation of bod pod for assessing body fat in collegiate football players. *Med Sci Sports Exerc.* 1999; 31:1350-6.
- Lockner DW, Heyward VH, Baumgartner RN, Jenkins KA. Comparison of air-displacement plethysmography, hydro densitometry, and dual X-ray absorptiometry for assessing body composition of children 10 to 18 years of age. *Ann NY Acad Sci.* 2000; 904:72-8.
- Fields DA, Goran MI, McCrory MA. Body- composition assessment via air-displacement plethysmography in adults and children: a review. *Am J Clin Nutr.* 2002;75(3):453-67.



- Pierson R, Wang J, Thornton J. Body composition comes of age: A modest proposal for the next generation. *Ann NY Acad Sci.* 2000; 904:1-11.
- Hangartner TN, Warner S, Braillon P, Jankowski L, Shepherd J. The official positions of the International Society for Clinical Densitometry: acquisition of dual-energy X-ray absorptiometry body composition and considerations regarding analysis and repeatability of measures. *J Clin Densitom.* 2013;16(4):520-36.
- Goodpaster BH. Measuring body fat distribution and content in humans. *Curr Opin Clin Nutr Metab Care.* 2002;5(5):481-7.
- Pietrobelli A, Wang Z, Formica C, Heymsfield SB. Dual-energy X-ray absorptiometry: fat estimation errors due to variation in soft tissue hydration. *Am J Physiol.* 1998;274(5 Pt 1): E808-16.
- Jackson AS, Pollock ML. Generalized equations for predicting body density of men. *Br J Nutr.* 1978; 40:497-504.
- Jackson AS, Pollock ML. A generalized equation for predicting body density of women. *Br J Nutr.* 1980; 12:175-81.
- Nevill AM, Metsios GS, Jackson AS, Wang J, Thornton J, Gallagher D. Can we use the Jackson and Pollock equations to predict body density/fat of obese individuals in the 21st century? *Int J Body Compos Res.* 2008;6(3):114-21.
- O'Connor DP, Bray MS, Mcfarlin BK, Sailors MH, Ellis KJ, Jackson AS. Generalized equations for estimating DXA percent fat of diverse young women and men: The TIGER Study. *Med Sci Sports Exerc.* 2010;42(10):1959-65.
- Lukaski HC, Johnson PE, Bolonchuk WW, Lykken GI. Assessment of fat-free mass using bioelectrical impedance measurements of the human body. *Am J Clin Nutr* 1985; 41:810-7.



- Kyle UG, Bosaeus I, De Lorenzo AD, Deurenberg P, Elia M, Gomez JM, et al. Bioelectrical impedance analysis—part I: a review of principles and methods. *Clin Nutr.* 2004; 23:1226-43.
- Das SK, Roberts SB, Kehayias JJ, Wang J, Hsu LKG, Shikora SA, et al. Body composition assessment in extreme obesity and after massive weight loss induced by gastric bypass surgery. *Am J Physiol Endocrinol Metab.* 2003;284(6): E1080-8.
- Flegal KM, Kit BK, Orpana H, Graubard BI. Association of all-cause mortality with overweight and obesity using standard body mass index categories: a systematic review and meta-analysis. *J Am Med Assoc.* 2013;309(1):71-82.
- Wang J, Thornton JC, Bari S, Williamson B, Gallagher D, Heymsfield SB, et al. Comparisons of waist circumferences were measured at 4 sites. *Am J Clin Nutr.* 2003; 77(2):379-384.